SAE INTERNATIONAL®

Characterization of Aging Effect on Three-Way Catalyst Oxygen Storage Dynamics

2016-01-0971
Published 04/05/2016

Stefano Sabatini and Irfan Kil
Clemson University

Travis Hamilton, Jeff Wuttke, Luis Del Rio, and Michael Smith
FCA US LLC

Zoran Filipi
Clemson University

Mark A. Hoffman
Clemson-ICAR

Simona Onori
Clemson University

CITATION: Sabatini, S., Kil, I., Hamilton, T., Wuttke, J. et al., "Characterization of Aging Effect on Three-Way Catalyst Oxygen Storage Dynamics," SAE Technical Paper 2016-01-0971, 2016, doi:10.4271/2016-01-0971.

Abstract

The Three Way Catalyst (TWC) is an effective pollutant conversion system widely used in current production vehicles to satisfy emissions regulations. A TWC's conversion efficiency degrades over time due to chemical and/or thermal mechanisms causing the catalyst to age. This reduction in conversion efficiency must be accounted for to ensure full useful life emissions compliance. This paper presents an experimental study of the aging impact on TWC performance. Four TWCs differentiated by their age, given in terms of miles driven, were tested. It is shown that the dynamics of oxygen storage are substantially affected by aging of the TWC. A previously developed physics-based oxygen storage model [1] is subsequently used to incorporate the effect of aging on the total Oxygen Storage Capacity (OSC). Parameter identification results for the different age catalysts show that total oxygen storage capacity decreases substantially with aging and is insensitive to operating conditions. This result allows the aging effect to be lumped into a single model parameter.

Introduction

The TWC is used for oxidation of hydrocarbons (HC), carbon monoxide (CO), and reduction of nitrogen oxides (NO_x) in production vehicles powered by SI engines. The ability to efficiently reduce exhaust gas emissions decreases over the lifetime of the TWC due to converter aging [3]. Aging is mainly caused by chemical and/or thermal mechanisms [4]. Chemical aging effects generally occur due to chemical compounds from engine oil additives and fuel such as sulfur (S), phosphorus (P), and lead (Pb). Poisoning, the main reason of chemical aging and TWC deactivation, results in washcoat surface fouling, decreasing oxidation rates and reduced TWC conversion efficiency [5]. Thermal aging results in reduced interaction between the precious metal and the exhaust gas due to the sintering of metal particles onto the washcoat itself, thus leading to decreased TWC conversion efficiency [6]. Figure 1 depicts the aging impact on TWC, "light off temperature" [1] and conversion efficiency [7]. It can be seen that thermal aging results in a significant increase of the "light off temperature" [7, 8]. The conversion efficiencies of exhaust gas pollutants (CO, NO and C_3H_8) decrease with aging, while "light off temperature" increases [7, 8].

TWC aging is a function of time and magnitude of exposure to elevated temperatures and chemical poisoning. Studies have been devoted to the development of accelerated aging methods with the purpose of aging a fresh catalyst within a short time to achieve simulated full useful life components that are similar to those obtained under real-world driving scenarios [9,10,11,12,13]. In particular, Ruetten et al., utilized a *rapid aging cycle* method to accelerate catalyst aging by inducing increased temperature at prescribed engine operating conditions [9]. The *laboratory scale method,* on the other hand, exposes the catalyst to accelerated chemical and/or thermal aging using an oven or a reactor.

1. "Light-off temperature" is defined as the temperature at which the catalyst conversion efficiency of CO reaches 50%.

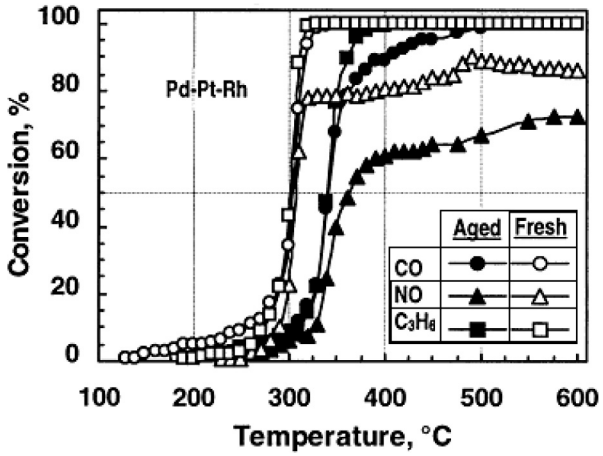

Figure 1. The effect of aging on a TWC conversion efficiency curve for CO, NO, and C_3H_8 [7]

Characterizing the dynamic behavior of the TWC is critical for controls studies. It is dominated by its ability to store and release oxygen. Earlier studies, [14, 15], have shown that the ceria surface area decreases with aging, which in turn decreases the TWC oxygen storage capacity (OSC).

A significant amount of research has been dedicated to identifying indicators that capture the effect of aging on the TWC [15,16,17,18,19]. A literature review reveals two primary methodologies: direct methods and indirect methods.

Direct methods are used to describe the aging effect on the catalyst via physical measurements at different aging levels. Detection of TWC aging with a microwave cavity perturbation in situ is a direct method example and was studied by Beulertz et al. [16]. In this work, the electrical properties of the catalyst coating were monitored via wire bound sensors or microwave antennas mounted inside the catalyst, and the resonance frequency was used as a direct index of catalyst aging. The drawback of this method is the complexity of the sensor layout and high cost. In [14, 15], the differences between CO-adsorbed and O_2-adsorbed, as measured by gas analyzer equipment, was used to calculate the OSC [14, 15]. Results from [15] demonstrate that OSC decreases with aging and is sensitive to temperature variations. Unfortunately, the identification of TWC OSC with these methods is expensive and time-consuming, and thus unsuitable for developing real-time models for on-board application.

Indirect methods, on the other hand, are based on OSC estimation [17,18,19]. In these studies, the dynamic behavior of the oxygen storage is represented through semi-empirical models, and the OSC estimation is obtained by evaluating the responses of the lambda sensors located upstream and downstream of the catalyst. However, the OSC estimated with these methods does not represent the physical storage capacity of the TWC. Rather, it is a representation of *phenomenological* oxygen storage capacity and is expressed as a function of temperature and exhaust mass flow rate [17, 18].Since OSC is an important parameter for characterizing the dynamic behavior of the TWC, the aging effect on the oxygen storage behavior needs to be investigated in detail. The major foci of this study are to: examine the aging effect on TWC oxygen storage, identify aging indicators, and determine whether the aging effect can be captured by a single model parameter.

We first describe the experimental setup used for data collection. Next, experimental results taken on four catalysts aged over different time durations are examined in terms of oxygen storage dynamics. Every catalyst is exposed to the same A/F ratio profile input, covering a range of square-wave amplitudes and frequencies, and the response of the post-catalyst lambda sensor is compared to pre-cat measurements. Analysis culminates in the proposition of indirect TWC aging indicators. The inclusion of the aging effect into the physics-based oxygen storage model is then presented. Finally, conclusions and future work are outlined.

Experiments

Experiments were performed in the chassis dynamometer test cell (Renk Labeco 4-wheel, 500HP Chassis Dyno) shown in Figure 2. The vehicle used in this investigation is a mid-size car utilizing a port fuel injected 3.6L V6 engine with 24 valves and a variable valve timing (VVT) mechanism.

The TWC used in the experiments was an instrumented, production, close-coupled catalyst consisting of two independent bricks in series, which are separated by a small gap and mounted in the same housing, as shown in Figure 3-a. The TWCs were made of monolithic structures of cordierite. More details about this type of catalyst can be found in Table 1.

Table 1. Geometric and structural specifications of the TWC

Specifications	Brick1	Brick 2
Length [mm]	68	68
Volume [l]	0.597	0.597
Cell density [cell/in^2]	600	400

The two-brick design allows for three measurement locations on the TWC, namely Pre-TWC, Mid-TWC and Post-TWC, as depicted in Figure 3. The Pre-TWC location quantifies the incoming exhaust gases via a wide range lambda sensor (λ_{pre_w}), a switch type lambda sensor (λ_{pre_s}) and a thermocouple (T_{pre}). The Mid-TWC location is also instrumented with a wide range lambda sensor (λ_{mid_w}), a switch type lambda sensor (λ_{mid_s}), and a thermocouple (T_{mid}). The Post-TWC is instrumented with one wide range lambda sensor (λ_{post_w}) and one thermocouple (T_{post}). Finally, the catalyst brick temperatures (T_{cat_1} and T_{cat_2}) are measured via thermocouples inserted to the flow centerline and 1.5 inches from the front face of each brick. The sensor schematic is shown in Figure 3-b. Thermocouples used for both exhaust gas and brick temperatures were all K-type. All wideband lambda sensors were Bosch LSU 4.9 with ECM F/A 1000 controllers.

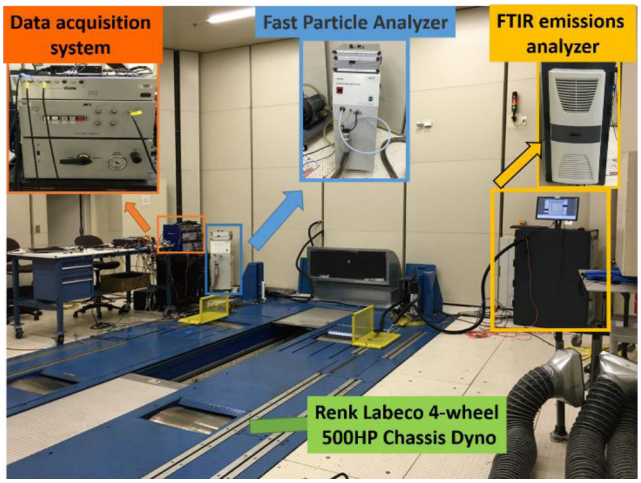

Figure 2. Chassis dynamometer test cell (Renk Labeco 4-wheel, 500HP Chassis Dyno) with specializes emission analyzers and a data acquisition system.

Tests were conducted using TWCs aged over four different time periods, varying from a green TWC to a full-useful-life TWC. Table 2 shows the history of each TWC with respect to equivalent miles. The green catalyst was fresh from production, with no intentional degreening. The "stock" catalyst arrived on the vehicle and had experienced approximately 20,000 miles of mixed cycle operation, without any accelerated aging. The "mid-life" catalyst underwent accelerated thermal aging representative of approximately 50,000 miles of real-world operation. Finally, the "OBD" catalyst underwent an aging procedure to represent a catalyst that is degraded well beyond the full useful life emissions standard.

Steady state experiments were conducted at six operating points with exhaust mass flow rates ranging from 10.2 g/s to 46.8 g/s. Table 3 summarizes the matrix of engine operating points. The same set of operating points was repeated with each of the four catalysts. Spark timing was utilized to create a tight distribution of exhaust gas temperatures at the catalyst inlet for all four catalysts that were previously aged to a different degree.

The lambda command profile used in the TWC tests is depicted in Figure 4. It comprises two separate sections. The first section consists of lambda amplitude variations (10% to 4% variation about the stoichiometric value). This section was formed to check the possible effect of lambda magnitude change on TWC dynamics.

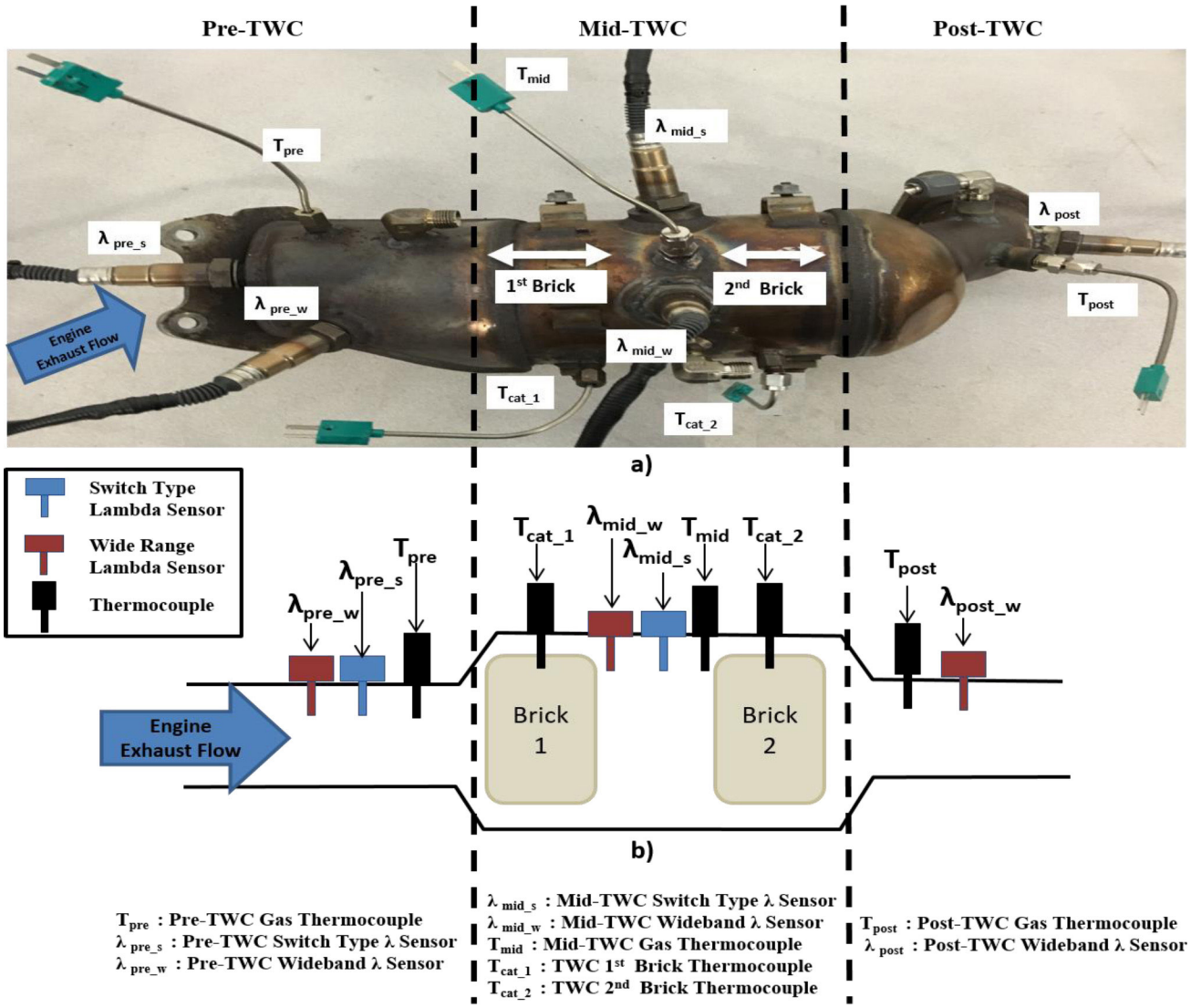

Figure 3. Instrumented TWC (a) and a schematic of the TWC sensor configuration (b)

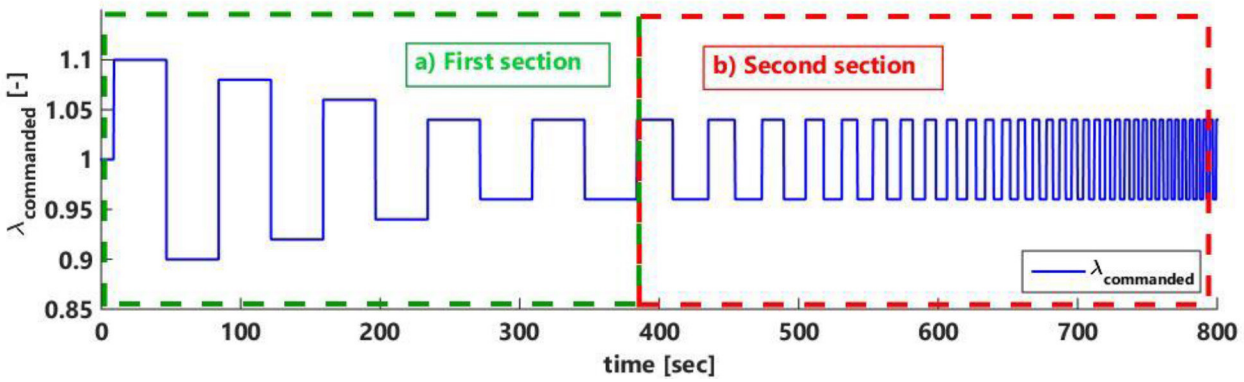

Figure 4. Lambda input profile used in the experiments: a) Varying amplitude lambda excursions (10% to 4% variation about stoichiometric value) with constant frequency b) Constant amplitude lambda excursions (4% variation about stoichiometric value) with varying frequency

Table 2. Catalyst history respect to miles driven

Catalyst	Aging Process	Distance [1000 Miles]
Green	--	0
Stock	On-road driving	20
Mid-life	Engine dyno aged with rapid aging cycle	50
OBD	OBD Aged	>150

The period of the commanded lambda step-change was selected such that complete catalyst oxygen filling and depletion is guaranteed for all four differently aged TWCs. Therefore, the oxygen storage capacity dynamics can be compared for differently aged TWCs.

The second section of the commanded lambda signal consists of a varying frequency, constant amplitude square-wave perturbation. The amplitude is 4% with respect to stoichiometry. This part was designed to observe the possible effect of square-wave period variation on the dynamic behavior of the TWC.

The experimental input profile is used for rendering changes to air fuel ratio control through INCA-ETAS. The desired air fuel ratio is generated in the Simulink/Matlab simulation environment and incorporated within INTECRIO. This process provides an automated and pre-programmed lambda alteration through INCA. Sensor signals were acquired through National Instruments cDAQ-9174 and 9205 ADC unit. Additionally, lambda signals were duplicated and brought into the INCA via ETAS ES930 I/O module for recording purposes.

Before commanding the lambda input profile, the vehicle was allowed to reach steady-state temperatures at all sensor locations for each combination of mass flow rate and engine load (Table 3). After reaching steady-state temperature, the vehicle was switched to open loop ETAS control and the lambda profile was commanded through adjustments to the injected fuel mass. Normalized Air-to-Fuel ratio was calculated from:

$$\lambda = \frac{(A/F)_{actual}}{(A/F)_{\text{stoichiometry}}} \quad (1)$$

where λ is the normalized air fuel ratio, $(A/F)_{actual}$ is the actual air to fuel ratio and $(A/F)_{stoichiometry}$ is the stoichiometric air to fuel ratio which is assumed to be 14.53 in this study.

Table 3. Testing conditions

Engine Speed [RPM]	Exhaust Mass Flow Rate [g/s]
1200	10.2
1500	14.4
1800	17.6
2200	23.6
2700	38.4
3200	46.8

Results & Discussion

An aging indicator can be derived from the lambda sensor responses upstream and downstream of the catalyst. The converter response to a lean to rich A/F step-change at 1500 rpm (14.4 g/s exhaust mass flow rate) is depicted in Figure 5 for the different TWCs considered. When the same lean to rich lambda excursion is applied at the TWC inlet, the time that λ_{post} takes to match λ_{pre} depends on the aging level. The time it takes for the pre and post lambda signals to match each other follows this trend: $t_{green} > t_{stock} > t_{mid\text{-}level} > t_{OBD}$.

The initial lean plateau is long enough to completely saturate the TWC with oxygen. After saturation, the lean to rich step change is applied. Because the rich exhaust gas lacks oxygen, the oxygen previously stored in the catalyst is used to oxidize the incoming HC and CO. Once the previously stored oxygen is fully consumed, the post-TWC lambda sensor will read rich as well, matching the pre-TWC lambda sensor. The fact that the depletion time decreases with the aging level suggests that a lesser amount of oxygen is stored in the converter as the catalyst ages. Therefore, we infer that the total Oxygen Storage Capacity for the catalyst considered in this work follows this trend $OSC_{green} > OSC_{stock} > OSC_{mid\text{-}life} > OSC_{OBD}$.

Since the real-time TWC oxygen storage capacity cannot be measured directly, it is important to estimate the oxygen storage capacity through a model relying only on the lambda sensor measurements. In the following, the oxygen storage model developed

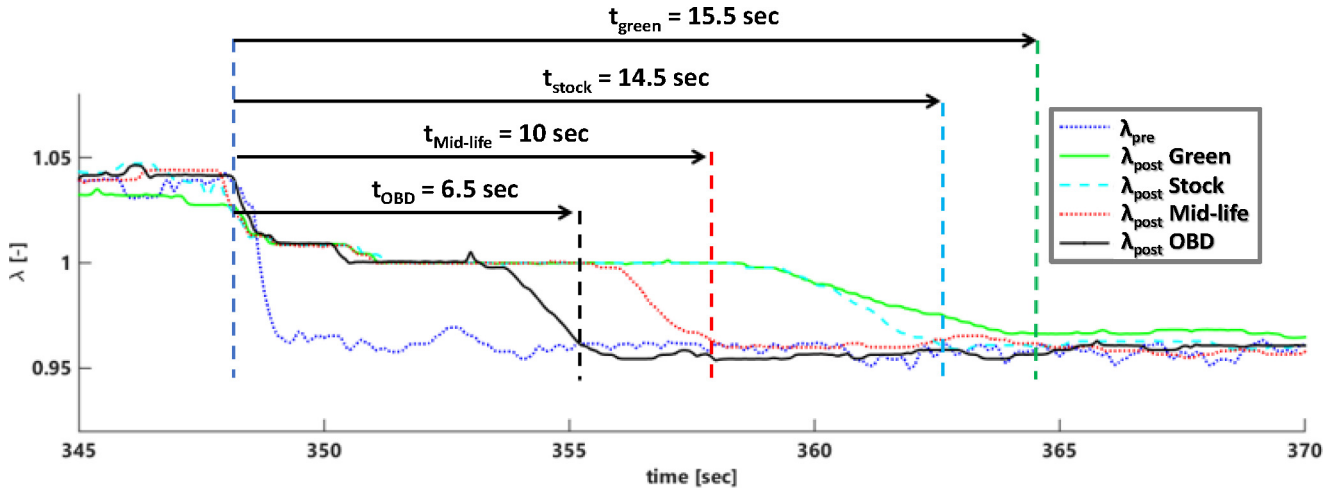

Figure 5. Effect of different aging level on the Oxygen Storage Dynamics of TWCs at 1500 rpm engine speed and 14.4 g/s exhaust mass flow rate. The time for the depletion phase of the each catalyst is depicted (t_{green} =15.5 > t_{stock}=14.5 > $t_{mid\text{-}life}$ =10> t_{OBD}=6.5).

in Kiwitz et al. [1] is briefly recalled, and a sensitivity study of the parameter representative of total oxygen storage capacity (OSC) with respect to converter aging is performed.

OSC Model

The oxygen storage dynamic model used in this paper is based on [1]. The simplified physics-based model utilizes only the chemical species crucial from an oxygen storage perspective. In particular, only one oxidizing gas species, O_2, and only one reducing gas species, CO, are considered. The oxygen storage capability of the converter is accounted by introducing two surface species, SO and S, that represent the oxidized and reduced form of ceria, respectively. Considering an Ely-Rideal mechanism, this is the resulting reaction scheme:

$$O_2 + 2S \rightleftharpoons 2SO \tag{2}$$

$$CO + SO \rightleftharpoons CO_2 + S \tag{3}$$

where (2) represents the oxygen absorption on the ceria and (3) the CO oxidation by the oxygen previously stored. Both the forward and backward reactions are considered resulting in the following net reactions rates that depend on the reactant concentrations:

$$r_1 = k_1^f [S]^2 [O_2] - k_1^b [SO]^2 c_0 \tag{4}$$

$$r_2 = k_2^f [SO][CO] - k_2^b [S][CO_2] \tag{5}$$

In the equation above, $[X]$ indicates the concentration of X chemical species in moles per m^3, c_o represents the total concentration in the exhaust gas and is defined as $c_o = P_{exh}/(RT_{pre})$ and k_i^f and k_i^b are the forward and backward reaction rate constants, respectively. The forward reaction constants depend on the catalyst temperature through the Arrhenius equation:

$$k_i^f = A_i \exp\left(-\frac{E_i}{RT_{cat}}\right) \tag{6}$$

Hence, in contrast with the majority of the semi-empirical models, the oxygen adsorption and desorption rates depend not only on the actual oxygen storage level $[SO]$ but also on the catalyst temperature [23]. The reduced and oxidized locations on the surface sum up to the total oxygen storage capacity OSC:

$$[SO] + [S] = OSC \tag{7}$$

The normalized oxygen storage level ϕ is considered:

$$\phi = [SO] / OSC \tag{8}$$

$$\frac{d\phi}{dt} = \frac{1}{OSC}(2r_1 - r_2) \tag{9}$$

The chemical species concentrations at the inlet of the TWC are estimated from the wide range lambda sensor measurements upstream of the catalyst (λ_{pre}) based on the air fuel definition presented in Auckenthaler et al. [24]. The model is suitable for real-time application in the vehicle, since the requested model inputs, λ_{pre}, T_{exh} and $\dot{m}_{exh}$, can be measured by commercially available sensors or easily estimated by the ECU.

Aging Inclusive Parameter Identification

The parameters to be identified for the oxygen storage are listed in Table 4 together with the equations in which they appear. The identification procedure finds the optimal set of parameters that minimizes the model error function J, defined as the root mean square of the difference between the simulated and measured lambda at the post/mid location during the transients illustrated in Figure 4.

$$J = RMS(error) = \sqrt{\frac{1}{N_{sample}} \sum_{k=1}^{N_{sample}} \left(\lambda_{meas}(k) - \lambda_{sim}(k)\right)^2} \quad (11)$$

A Particle Swarm Optimization (PSO) algorithm, [25], was used for the parameter value search. A different OSC value was identified for each operating point. Using the parameters found with this procedure, the root mean square error (RMSE) of the model is lower than 7% for all operating points tested.

Table 4. Parameters to be identified for Oxygen Storage Model

Parameters	Description	Equation
$A1$ $E1$	k_i^f Arrhenius parameters	$k_1^f = A_1 \exp(-\frac{E_1}{RT_{cat}})$
$A2$ $E2$	k_i^f Arrhenius parameters	$k_2^f = A_2 \exp(-\frac{E_2}{RT_{cat}})$
a b c	Nobel Metal Gibbs energy parameters	$\Delta G = \frac{a + bT_{cat}}{c + T_{cat}}$
OSC [mol/m^3]	Oxygen storage capacity	$\frac{d\Phi}{dt} = \frac{1}{OSC}(2r_1 - r_2)$

Figure 6 presents the identified OSC values for the first and second bricks, respectively. Note that all parameters other than OSC from Table 4 are held constant. OSC values are normalized with respect to maximum value identified for each brick. First, it can be noticed how the oxygen storage capacity dramatically decreases with aging (see Figure 7). Note that the oxygen storage capacity presented here is an indirect normalized measure of the real oxygen storage capacity, identified by fitting the model simulation to experimental data. Therefore the absolute capacity magnitudes are strongly related to the model used during the identification procedure.

Furthermore, with the exception of the Green catalyst, whose temperature behavior is in contrast to other TWC ages, the identified oxygen storage capacities are found to be insensitive to operating conditions. This is in apparent contrast with the approach presented in Balenovic et al. [17] where a strong dependence of the total oxygen storage capacity to temperature and flow rate is considered in the model. However, the model used in this work includes a physic-based, temperature dependent reaction scheme, equation 6 [23]. The apparent contradiction is explained by the fact that temperature effects are already included in the reaction rates. While the normalized oxygen storage level, ϕ, will vary with temperature, the total oxygen storage capacity is nearly constant for any single TWC age. This is an important result from a control and diagnostic perspective since it shows that the TWC aging effect can be captured by a single model parameter insensitive to the operating condition that can be identified online using a proper estimation strategy.

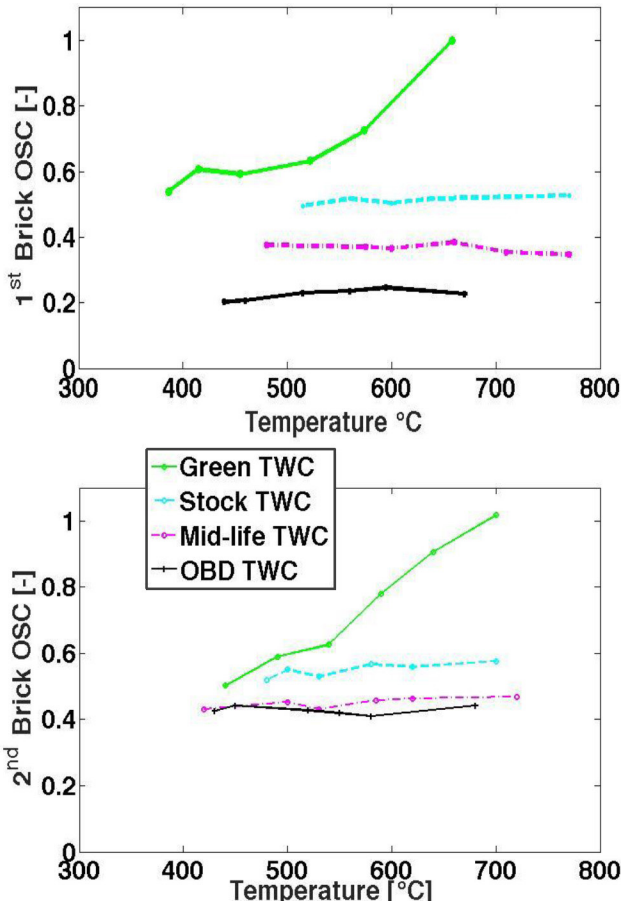

Figure 6. Identification results of normalized OSC values relative to the a) first brick of OSC b) second brick of OSC for the green and aged catalysts, and all operating points.

Table 5. Average normalized OSC values for the catalysts used in this work

Parameter	Catalyst	First Brick	Second Brick
OSC[-]	Green	1	1
	Stock	0.75	0.75
	Mid-life	0.52	0.61
	OBD	0.33	0.58

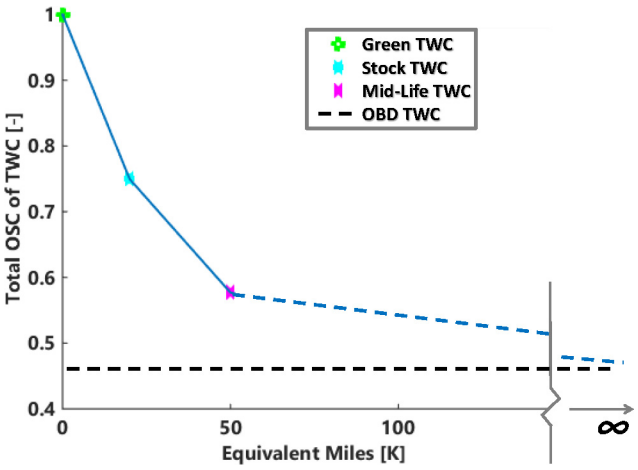

Figure 7. Total normalized mean value of OSC for both bricks versus equivalent miles traveled. Values apply to all operating points of green and aged catalysts.

Conclusion

In this paper, the effects of aging on TWC oxygen storage are presented and the post lambda sensor response is proposed as an aging indicator. Furthermore, a study of how the aging effect can be incorporated in a previously developed TWC model is performed. Results showed that the identified OSC parameter of the TWC model decreases with age and is insensitive to temperature. Future works will characterize the effect of lambda changes of varying amplitude and frequency on the oxygen storage dynamics, the model validation under real driving conditions and the design of a proper online adaptation strategy for the OSC parameter.

References

1. Kiwitz, P., Onder, C., Guzzella, L., "Control-oriented modeling of a three-way catalytic converter with observation of the relative oxygen level profile." Journal of Process Control 22 : 984-994 ,2012, doi:10.1016/j.jprocont.2012.04.014
2. 'EPA and NHTSA Set Standards to Reduce Greenhouse Gases and Improve Fuel Economy for Model Years 2017-2025 Cars and Light Trucks', Regulatory Announcement, United States Environmental Protection Agency, Office of Transportation and Air Quality, Washington, DC, USA, August 2012
3. Matam, S.K., Otal, E. H., Aguirre, M. H. , Winkler, A., Ulrich, A., Rentsch, D., Weidenkaff, A., and Ferri, D.. "Thermal and chemical aging of model three-way catalyst Pd/Al 2 O 3 and its impact on the conversion of CNG vehicle exhaust." Catalysis Today 184, no. 1 : 237-244, 2012 doi:10.1016/j.cattod.2011.09.030
4. Peterson, E.E., Bell, A.T., Catalyst Deactivation, Marcel-Dekker, New York, 1987
5. Moldovan, M., Rauch, S., Morrison, G.M., Gomez, M., and Palacios, M.A.. "Impact of ageing on the distribution of platinum group elements and catalyst poisoning elements in automobile catalysts."Surface and interface analysis 35, no. 4 (2003): 354-359. doi:10.1002/sia.1541
6. Cooper, B.J., "Durability of platinum-containing automotive exhaust control catalysts", Platinum Metals Rev 27, no. 4 (1983): 146-155.
7. González-Velasco, J. R., Botas, J.A., Ferret, R.,"Thermal aging of Pd/Pt/Rh automotive catalysts under a cycled oxidizing-reducing vironment." Catalysis today 59, no. 3 (2000): 395-402 doi:10.1016/S0920-5861(00)00304-7
8. Winkler, A., Ferri, D. and Hauert, R. "Influence of aging effects on the conversion efficiency of automotive exhaust gas catalysts."Catalysis Today 155.1 (2010): 140-146. doi:10.1016/j.cattod.2008.11.021
9. Ruetten, O., Pischinger, S., Küpper, C., Weinowski, R. et al., "Catalyst Aging Method for Future Emissions Standard Requirements," SAE Technical Paper 2010-01-1272, 2010, doi:10.4271/2010-01-1272.
10. Granados, M. L., Galisteo, F. C., Mariscal, R., Alifanti, M., Gurbani, A., Fierro, J.L., Fernández-Ruíz, R., "Modification of a three-way catalyst washcoat by aging: A study along the longitudinal axis." Applied surface science 252, no. 24 (2006): 8442-8450. doi:10.1016/j.apsusc.2005.11.053
11. Andersson, J., Antonsson, M., Eurenius, L., Olsson, E., and Skoglundh, M., "Deactivation of diesel oxidation catalysts: Vehicle-and synthetic aging correlations." Applied Catalysis B: Environmental 72, no. 1 (2007): 71-81. doi:10.1016/j.apcatb.2006.10.011
12. Ramanathan, K., and Se H. Oh. "Modeling and analysis of rapid catalyst aging cycles." Chemical Engineering Research and Design 92, no. 2 (2014): 350-361. doi:10.1016/j.cherd.2013.06.020
13. Koltsakis, G. C., and Stamatelos, A. M., "Catalytic automotive exhaust aftertreatment." Progress in Energy and Combustion Science 23, no. 1 (1997): 1-39. doi:10.1016/S0360-1285(97)00003-8
14. Kallinen, K., Suopanki, A., and Härkönen Matti. "Laboratory scale simulation of three-way catalyst engine ageing." Catalysis today 100.3 (2005): 223-228. doi:10.1016/j.cattod.2004.09.057
15. Maunula, T., Vakkilainen, A., Lievonen, A., Torkkell, K. et al., "Low Emission Three-way Catalyst and OSC Material Development for OBD Diagnostics," SAE Technical Paper 1999-01-3625, 1999, doi:10.4271/1999-01-3625.
16. Beulertz, G., Votsmeier, M., Moos, R., "In operando detection of three-way catalyst aging by a microwave-based method: Initial studies."Applied Sciences 5, no. 3 (2015): 174-186. doi:10.3390/app5030174
17. Balenovic, M., Backx, T., and de Bie, T., "Development of a Model-Based Controller for a Three-Way Catalytic Converter," SAE Technical Paper 2002-01-0475, 2002, doi:10.4271/2002-01-0475.
18. Ingram, G. and Surnilla, G., "On-line Oxygen Storage Capacity Estimation of a Catalyst," SAE Technical Paper 2003-01-1000, 2003, doi:10.4271/2003-01-1000.
19. Peyton Jones, J. and Muske, K., "Model-based OBD for Three-Way Catalyst Systems," SAE Technical Paper 2004-01-0639, 2004, doi:10.4271/2004-01-0639.
20. Torcrona, A., Skoglundh, M., Thormahlen, P., Fridell, E., Jobson, E., "Low temperature catalytic activity of cobalt oxide and ceria promoted Pt and Pd: -influence of pretreatment and gas composition," Applied Catalysis 14, p. 131-146, 1997, doi:10.1016/S0926-3373(97)00018-0
21. Yee, A., Morrison, S.J., Idriss, H., "A Study of the Reactions of Ethanol on CeO2 and Pd/CeO2 by Steady State Reactions, Temperature Programmed Desorption, and In Situ FT-IR," Journal of Catalysis 186, p. 279-295, 1999, doi:10.1006/jcat.1999.2563
22. McAtee, C., McCullough, G., Douglas, R., and Glover, L., "The Effect of De-Greening and Pre-Treatment on Automotive Catalyst Performance," SAE Technical Paper 2011-24-0188, 2011, doi:10.4271/2011-24-0188.
23. Sabatini, S., Kil, I., Dekar, J., Hamilton, T., Wuttke, J., Smith, M., Hoffman, M., Onori, S., "A New Semi-Empirical Temperature Model for the Three Way Catalytic Converter." *IFAC-PapersOnLine* 48, no. 15 (2015): 434-440. doi:10.1016/j.ifacol.2015.10.062
24. Auckenthaler, T. S., Modelling and control of three-way catalytic converters. Diss., Technische Wissenschaften, Eidgenössische Technische Hochschule ETH Zürich, Nr. 16018, 2005, 2005.

25. Soren, E., Kiwitz, P., and Guzzella, L., "A generic particle swarm optimization Matlab function." In American Control Conference (ACC), 2012, pp. 1519-1524. IEEE, 2012. doi:10.1109/ACC.2012.6314697

Definitions/Abbreviations

c_o - Total concentration in the gas

CO - Carbon monoxide

EPA - Environmental Protection Agency

HC - Hydrocarbon

NO_x - Generic term for mono-nitrogen oxides NO and NO_2

OBD - On-board diagnostics

OSC - Oxygen Storage Capacity

O_2 - Oxygen

P_{exh} - Exhaust gas pressure

P - Chemical symbol for the element phosphorus

Pb - Chemical symbol for the element lead

R - Gas Constant

S - Chemical symbol for the element sulfur

TWC - Three Way Catalyst

T_{cat1} - TWC 1st Brick Thermocouple

T_{cat2} - TWC 2nd Brick Thermocouple

T_{mid} - Pre-TWC Gas Thermocouple

T_{post} - Post-TWC Gas Thermocouple

T_{pre} - Pre-TWC Gas Thermocouple

λmid_s - Mid-TWC Switch-type λ sensor

λmid_w - Mid-TWC Wideband λ sensor

λpre_s - Pre-TWC Switch-type λ sensor

λpre_w - Pre-TWC Wideband λ sensor

λpost_w - Post-TWC Wideband λ sensor

The Engineering Meetings Board has approved this paper for publication. It has successfully completed SAE's peer review process under the supervision of the session organizer. The process requires a minimum of three (3) reviews by industry experts.

ISSN 0148-7191

http://papers.sae.org/2016-01-0971